Radiomics-based prediction of HCC response to atezolizumab/bevacizumab

ISAAC RODRIGUEZ[1], ABHINAY VELLALA[2], TIMO ITZEL[1], JIMMY DAZA[1], MICHAEL VÁCHA[1], DE-HUA CHANG[3,4], MANUEL DEBIC[4], MICHAEL T. DILL[5-7], MAX SEIDENSTICKER[8], JULIA MAYERLE[9], STEFAN MUNKER[9], STEFAN O. SCHOENBERG[2], LUKAS MÜLLER[10], PETER R. GALLE[11], ARNDT WEINMANN[11], DIETMAR TAMANDL[12], MATTHIAS PINTER[13], BERNHARD SCHEINER[13], CHRISTEL WEISS[14], MACIEJ PECH[15], FRIEDRICH SINNER[16], VERENA KEITEL[16], MARINO VENERITO[16], MATTHIAS PHILIP EBERT[17-20], ANDREAS TEUFEL[1,17,19*] and MATTHIAS F. FROELICH[2*]

[1]Division of Hepatology, Division of Clinical Bioinformatics, Department of Medicine II, Medical Faculty Mannheim, Heidelberg University, D-68167 Mannheim, Germany; [2]Department of Radiology and Nuclear Medicine, Medical Faculty Mannheim, Heidelberg University, D-68167 Mannheim, Germany; [3]Department of Radiology, Cantonal Hospital of Lucerne, 6000 Lucerne, Switzerland; [4]Department of Radiology, Medical Faculty Heidelberg, Heidelberg University, D-69120 Heidelberg, Germany; [5]Department of Gastroenterology, Hepatology, Infectious Diseases and Intoxications, Heidelberg University Hospital, D-69120 Heidelberg, Germany; [6]National Center for Tumor Diseases, National Center for Tumor Diseases Heidelberg, a Partnership Between German Cancer Research Center and Heidelberg University Hospital, D-69120 Heidelberg, Germany; [7]German Cancer Research Center Heidelberg, Research Group Experimental Hepatology, Inflammation and Cancer, D-69120 Heidelberg, Germany; [8]Department of Radiology, University Hospital, Ludwig-Maximilians-Universität Munich, D-80336 Munich, Germany; [9]Department of Medicine II, University Hospital, Ludwig-Maximilians-Universität Munich, D-80336 Munich, Germany; [10]Department of Diagnostic and Interventional Radiology, University Medical Center Mainz, Mainz University, D-55131 Mainz, Germany; [11]University Medical Center I, Department of Medicine, Mainz University, D-55131 Mainz, Germany; [12]Department of Radiology, Medical Faculty Vienna, Vienna University, A-1090 Vienna, Austria; [13]Division of Gastroenterology and Hepatology, Department of Medicine III, Medical University of Vienna, A-1090 Vienna, Austria; [14]Department of Medical Statistics, Biomathematics and Information Processing, Medical Faculty Mannheim, Heidelberg University, Mannheim, Germany; [15]Department of Radiology and Nuclear Medicine, Magdeburg University, D-39120 Magdeburg, Germany; [16]Department of Gastroenterology, Hepatology and Infectious Diseases, Medical Faculty Magdeburg, Magdeburg University, D-39120 Magdeburg, Germany; [17]Department of Medicine II, Medical Faculty Mannheim, Heidelberg University, D-68167 Mannheim, Germany; [18]German Cancer Research Center Hector Cancer Institute at University Medicine Mannheim, Medical Faculty Mannheim, Heidelberg University, D-68167 Mannheim, Germany; [19]Clinical Cooperation Unit Healthy Metabolism, Center for Preventive Medicine and Digital Health, Medical Faculty Mannheim, Heidelberg University, D-68167 Mannheim, Germany; [20]Molecular Medicine Partnership Unit, European Molecular Biology Laboratory, D-69117 Heidelberg, Germany

Received September 6, 2024; Accepted October 30, 2024

DOI: 10.3892/ol.2025.15229

Abstract. Advanced hepatocellular carcinoma (HCC) treatment has evolved with the introduction of atezolizumab/bevacizumab, showing improved outcomes over sorafenib. However, the response varies among patients, particularly between viral and non-viral etiologies. The present study aimed to develop and evaluate multimodal prediction models combining quantitative imaging and clinical markers to predict the treatment response in patients with HCC. Between March 2020 and May 2023, patients with advanced HCC treated with atezolizumab/bevacizumab were retrospectively identified from six centers in Germany and Austria. Patients underwent baseline contrast-enhanced liver MRI and follow-up imaging to assess the therapy response. Machine learning models, including RandomForestClassifier, were developed for radiomics, clinical and combined datasets. Hyperparameter tuning was performed using RandomizedSearchCV, followed by cross-validation to evaluate model performance. The study included 103 patients, with 70 achieving disease control (DC)

Correspondence to: Professor Andreas Teufel, Division of Hepatology, Division of Clinical Bioinformatics, Department of Medicine II, Medical Faculty Mannheim, Heidelberg University, Theodor-Kutzer-Ufer 1-3, D-68167 Mannheim, Germany
E-mail: teufel@medma.uni-heidelberg.de

*Contributed equally

Key words: radiomics, machine learning, hepatocellular carcinoma, prediction models, checkpoint inhibitors

and 33 experiencing disease progression (PD). Key findings included significant differences in treatment response and progression-free survival between the DC and PD groups. The radiomics model, using 14 selected features, achieved 73.1% accuracy and a receiver operating characteristic (ROC) area under the curve (AUC) of 0.635 for the test set. The clinical model, with 4 selected features, achieved 73% accuracy and a ROC AUC of 0.649 for the test set. The combined model showed improved performance, with 69% accuracy and a ROC AUC of 0.753 for the test set. Hyperparameter tuning further enhanced the accuracy of the combined model to 80.1% and the ROC AUC to 0.771 for the test set. In conclusion, the hybrid model combining clinical and radiological data outperformed individual models, providing improved predictions of response to atezolizumab/bevacizumab in patients with HCC.

Introduction

Hepatocellular carcinoma (HCC) stands as a significant contributor to the global cancer burden, representing 75-85% of all primary liver cancers, making it the most common liver malignancy (1). HCC typically originates from liver cirrhosis, which can be caused by various chronic liver diseases such as metabolic dysfunction-associated steatotic liver disease, alcohol-related liver disease, hepatitis B virus (HBV), and hepatitis C virus (HCV) infection (2).

Therapeutic options for HCC vary based on size and location and are guided according to the Barcelona Clinic Liver Cancer System (BCLC) (3,4). Small nodules may be treated with liver transplantation, surgical resection, or local ablation, while larger or multiple nodules confined to the liver often undergo transarterial chemoembolization (TACE). Advanced or extrahepatic tumors (BCLC-C) typically require systemic therapy (4-6).

Until 2020, sorafenib was the main systemic treatment for advanced HCC. However, the IMbrave150 trial showed that atezolizumab/bevacizumab, a combination of targeted immunotherapy, significantly improved survival and tumor response compared to sorafenib alone, leading to its recommendation as the first-line treatment for BCLC-C patients (4,7-10). Nevertheless, a subgroup analysis from the IMbrave150 data revealed that patients with non-viral etiology may not benefit as much from atezolizumab/bevacizumab compared to sorafenib (11). Thus, while some patients may derive significant benefit from atezolizumab/bevacizumab, others may not. As a result, to streamline patients' treatment, the prediction of response would be very beneficial-particularly with the recent approval of alternative immunotherapies and further positive phase III clinical trials (12-14). Therefore, this study aimed to investigate multimodal prediction models, consisting of quantitative imaging and clinical markers.

Materials and methods

Patient collective. From March 2020 to May 2023, patients aged 18 years and older with hepatocellular carcinoma stadium BCLC-C (advanced), BCLC-B (intermediate, not suitable for locoregional therapy) or BCLC-A and D (with a justifiable reason to start immunotherapy), regardless of comorbidities or previous treatments, were retrospectively identified from six different centers in Germany (Mannheim, Heidelberg, Munich, Magdeburg, Mainz) and Austria (Vienna). Two inclusion criteria were crucial: treatment with atezolizumab/bevacizumab and baseline dedicated contrast-enhanced liver MRI (at least T2, DWI, and T1 Contrast Dynamic). For analysis, the venous phase from the contrast-enhanced dynamic MRI was employed. Also, all included MRIs were read for adequate image quality by a board-certified radiologist before inclusion in the study. Additionally, patients must have undergone a second radiological evaluation (either MRI or CT) to determine response to therapy after at least three months of atezolizumab/bevacizumab, according to the modified Response Evaluation Criteria on Solid Tumors (mRECIST) (15). Based on this, the cohort was divided into a disease control (DC) group or a progressive disease (PD) group. DC encompasses patients of the mRECIST categories complete response (CR), partial response (PR), and stable disease (SD). Relevant clinical information was retrieved, including age, sex, etiology, previous therapy, ECOG performance status, Child-Pugh Score, and laboratory values, as well as survival data, to perform progression-free and overall survival analysis.

Statistical analysis. The statistical analysis was performed in R version 4.1.2. For quantitative variables that were approximately normally distributed, the mean and standard deviation were calculated. For non-normally distributed data, the median and interquartile range are presented. For categorical variables, frequencies and percentages are presented. Comparison of quantitative variables between two groups was performed using an unpaired two-sample t-test or a Mann-Whitney U test for non-normally distributed data. Fisher's exact test was used to compare the proportions of categorical variables between groups. Survival analysis was conducted using the Kaplan-Meier method, with log-rank tests to compare the survival distributions between different groups. Each test was conducted as a two-sided test. $P<0.05$ was considered to indicate a statistically significant difference.

Tumor segmentation and feature extraction. The baseline MRI was utilized to extract radiomics features, specifically the late portal venous phase, where the washout phenomenon can be observed. For this purpose, segmentation of the region of interest (ROI), defined as the biggest tumor lesion in each patient, was performed by a physician (I.R., with two years of experience in segmentation) and evaluated and corrected by a clinical radiologist (M.F., with five years of experience in oncologic imaging) in a semi-automated fashion using 3D Slicer (version 4.10.2) (16). Before feature extraction, preprocessing steps were applied to ensure comparability of the images between the different centers; this included bias field correction, intensity normalization, and image resampling.

Radiomics feature extraction was conducted in Python version 3.11. using pyradiomics (17). The feature extractor was configured with a bin count of 32, 'sitkBSpline' as an interpolation method, and resampled pixel spacing [1, 1, 1]. The following features were extracted: first-order, shape, GLCM (gray level co-occurrence matrix), GLDM (gray level dependence matrix), GLRLM (gray level run length matrix), GLSZM (gray level size zone matrix), and NGTDM (neighboring gray-tone difference matrix).

Feature selection and machine-learning model development. Both clinical variables and extracted radiomics features were standardized using MinMaxScaler. To select the relevant features, a pipeline using the SelectKBest method with the f_classif scoring function was implemented. This process was iterated over a range of k values (2 to 50 for radiomics data, and 2 to 21 for the clinical data) to determine the optimal number of features that yield the best model performance. To develop the predictive model a RandomForestClassifier with entropy criterion, max depth of 10, and 2 estimators was chosen for its balance between complexity and interpretability. The classifier was trained and tested using a stratified 75/25 train-test split to maintain class distribution balance, considering 70 patients in the DC group and 33 in the PD group. For each k value, the model's performance was evaluated using accuracy and ROC AUC scores on both training and test datasets. A radiomics and clinical model were independently designed and then joined into the combined model.

Hyperparameter tuning was conducted using RandomizedSearchCV. The parameter grid included: the number of trees in the forest (2, 3, 5), the number of features to consider at each split ('log2', 'sqrt'), the maximum number of levels in each tree (2, 3, 5, None), minimum number of samples required to split a node (2, 3, 4), a minimum number of samples required at each leaf node (1, 2, 4), bootstrap sampling (True, False), and the criterion for the quality of a split ('entropy', 'gini', 'log_loss'). RandomizedSearchCV was run with 500 iterations using an 18-fold cross-validation. The combined model was trained using these parameters and reevaluated on both training and testing sets.

Results

Baseline characteristics. A total of 103 patients from six different centers were included. Among them, 70 patients achieved disease control (DC group) while 33 experienced disease progression (PD group) during treatment with atezolizumab/bevacizumab.

The etiology of HCC varied among patients in the DC group, with alcohol (30.0%), viral etiology (17.1%), and NASH/NAFLD (28.6%) being the most common. Cirrhosis was present in 81.4% of patients, and the majority had no signs of decompensation. Most patients exhibited no signs of hepatic encephalopathy (97.1%) and had mild to moderate ascites. In comparison, in the PD group, the viral etiology had a higher proportion (33%) than alcoholic (21%), however, this difference was not statistically significant. Cirrhosis was less prevalent (69%) with a higher frequency of refractory ascites (18%), but again, without a significant difference.

Regarding the line of treatment, the majority of patients responding to atezolizumab/bevacizumab were undergoing their first-line treatment (91.4% in the DC group vs. 63.5% in the PD group, P=0.003). Previous treatment had been received by 58.6% of patients in the DC group, with surgical resection (18.6%) and transarterial chemoembolization (TACE) (35.7%, P=0.038) being the most common interventions, TACE being slightly significant. In the PD group, the proportion of patients who received systemic therapy was significantly higher (8.6% in the DC group vs. 33.3% in the PD group, P=0.003).

The baseline laboratory parameters showed comparable values between the two groups, with no significant differences in liver function as bilirubin, albumin, and international normalized ratio (INR) were comparable among different groups. Also, creatinine and alpha-fetoprotein (AFP) levels did not differ significantly. However, significant differences were observed in C-reactive protein (CRP) levels (P=0.001).

Other notable findings include the distribution of BCLC stage, as in the PD group more patients were diagnosed with BCLC stage C cancers (81.8% in the PD group vs. 60% in the DC group). However, this difference was not considered statistically significant. Also, more patients in the PD group suffered from distant metastases of the disease (60.6% in the PD group vs. 34.3% in the DC group, P=0.018). Complete baseline parameters are shown in Table I.

Response to therapy and survival. The primary outcomes of interest were disease control and progression-free survival (PFS). As a proof of principle, patients in the DC group exhibited better response rates and prolonged PFS compared to those in the PD group. Specifically, in the DC group, 5.7% of patients achieved a complete response, 32.9% achieved a partial response, and 61.4% exhibited stable disease (Fig. 1).

The disparities in treatment response and PFS were reflected in lower overall survival rates and increased mortality rates between the two groups. Patients in the DC group experienced a longer median progression-free survival of 280.50 days [interquartile range (IQR): 169.00-445.25], in contrast to 81.00 days (IQR: 56.00-89.00) in the PD group. Similarly, patients with favorable treatment responses had a longer median overall survival of 381.50 days (IQR: 226.75-568.50), compared to 147.00 days (IQR: 90.00-309.00) in the other group. Additionally, the mortality rate was lower in patients with favorable treatment responses, with 32.9% experiencing mortality compared to 63.6% in the other group (Table II).

The primary reason for discontinuing therapy was radiological progression after three months of atezolizumab/bevacizumab treatment (Table II). Consequently, patients in the PD group received a significantly lower median number of treatment cycles, with a median of 4.00 cycles (IQR: 3.00-5.00), compared to 10.00 cycles (IQR: 6.00-17.50) in the other group (P<0.001) (Table I).

Patients in the PD group had a lower prevalence of immune related adverse events (irAEs) (Table SI).

Feature selection and model development

Radiomics model. A total of 103 tumor segmentations were performed (Fig. 2). From each segmentation, 107 radiomics features were obtained. For the radiomics model, 14 features were selected (Fig. 3A), including: first order (Skewness) GLSZM (Large Area Low Gray Level Emphasis, Zone Variance, Large Area High Gray Level Emphasis, Large Area Emphasis, Low Gray Level Zone Emphasis) GLCM (Cluster Shade, Joint Average, Autocorrelation, Sum Average) GLRLM (Short Run High Gray Level Emphasis, Long Run Low Gray Level Emphasis, High Gray Level Run Emphasis), GLDM (High Gray Level Emphasis). The training set showed an accuracy of 80.5% and a ROC AUC of 0.9212 to predict progression (PD group), with 60% sensitivity and 90.4% specificity. The test set exhibited an accuracy of 73.1% and a ROC AUC of 0.6354, with 37.5% sensitivity and 88.9% specificity (Fig. 4A).

Clinical model. The optimal k value for clinical features was determined to be 4. The selected features were: C-reactive

Table I. Overview of baseline characteristics of all patients with hepatocellular carcinoma treated with atezolizumab and bevacizumab.

Characteristics	Disease control (n=70)	Progressive disease (n=33)	P-value
Center, n (%)			0.004[a]
Heidelberg	25 (35.7)	12 (36.4)	
Mainz	2 (2.9)	5 (15.2)	
Mannheim	4 (5.7)	8 (24.2)	
Magdeburg	21 (30.0)	3 (9.1)	
Munich	9 (12.9)	2 (6.1)	
Vienna	9 (12.9)	3 (9.1)	
Median age, years (IQR)	70.50 (62.00, 76.75)	68.00 (60.00, 72.00)	0.224
Sex (female), n (%)	17 (24.3)	8 (24.2)	>0.999
Mean height (SD)	173.10 (9.53)	173.61 (8.54)	0.796
Mean weight (SD)	84.00 (15.56)	84.79 (16.07)	0.813
Etiology, n (%)			0.152
Alcohol	21 (30.0)	7 (21.2)	
Viral	12 (17.1)	11 (33.3)	
NASH/NAFLD	20 (28.6)	4 (12.1)	
Other[b]	7 (10.0)	5 (15.2)	
Unknown	10 (14.3)	6 (18.2)	
Cirrhosis (yes), n (%)	57 (81.4)	23 (69.7)	0.210
Hepatic encephalopathy, n (%)			0.390
None	68 (97.1)	32 (97.0)	
Mild	0 (0.0)	1 (3.0)	
Severe	2 (2.9)	0 (0.0)	
Ascites, n (%)			0.085
No diuretics	32 (45.7)	18 (54.5)	
Diuretics	33 (47.1)	9 (27.3)	
Refractory	5 (7.1)	6 (18.2)	
Previous treatment (yes), n (%)	41 (58.6)	22 (66.7)	0.518
Resection (yes), n (%)	13 (18.6)	11 (33.3)	0.134
RFA (yes), n (%)	13 (18.6)	2 (6.1)	0.135
TACE (yes), n (%)	25 (35.7)	5 (15.2)	0.038[a]
Radiation (yes), n (%)	2 (2.9)	1 (3.0)	>0.999
SIRT (yes), n (%)	9 (12.9)	1 (3.0)	0.162
Systemic therapy (yes), n (%)	6 (8.6)	11 (33.3)	0.003[a]
Line of treatment atezolizumab/ bevacizumab, n (%)			0.003[a]
First	64 (91.4)	21 (63.6)	
Second	2 (2.9)	5 (15.2)	
Third	2 (2.9)	5 (15.2)	
Fourth	2 (2.9)	2 (6.1)	
Median cycles (IQR)	10.00 (6.00, 17.50)	4.00 (3.00, 5.00)	<0.001[a]
Median bilirubin (IQR)	0.88 (0.60, 1.54)	1.00 (0.60, 1.40)	0.832
Median albumin (IQR)	28.10 (4.15, 37.22)	29.00 (4.30, 33.60)	0.813
Mean quick test (SD)	81.47 (17.18)	78.18 (21.88)	0.463
Median INR (IQR)	1.12 (1.03, 1.20)	1.17 (1.08, 1.29)	0.347
Median CRP (IQR)	2.00 (0.49, 7.60)	6.50 (4.00, 10.60)	0.001[a]
Median Na^+ (IQR)	138.00 (136.00, 139.00)	139.00 (137.00, 141.00)	0.041[a]
Median Cr (IQR)	0.85 (0.71, 1.08)	0.84 (0.70, 1.28)	0.532
Median AFP (IQR)	43.56 (8.38, 631.00)	99.90 (4.90, 5047.00)	0.912

Table I. Continued.

Characteristics	Disease control (n=70)	Progressive disease (n=33)	P-value
Child-Pugh stage, n (%)			0.336
A	55 (78.6)	23 (69.7)	
B	15 (21.4)	10 (30.3)	
C	0 (0.0)	0 (0.0)	
ECOG, n (%)			0.211
0	43 (61.4)	15 (45.5)	
1	25 (35.7)	17 (51.5)	
2	2 (2.9)	1 (3.0)	
Macrovascular invasion (yes), n (%)	17 (24.3)	13 (39.4)	0.163
Metastasis (yes), n (%)	24 (34.3)	20 (60.6)	0.018
BCLC stadium, n (%)			0.130
A	1 (1.4)	0 (0.0)	
B	21 (30.0)	4 (12.1)	
C	42 (60.0)	27 (81.8)	
D	6 (8.6)	2 (6.1)	

[a]Statistically significant (P<0.05). [b]Includes primary biliary cirrhosis, primary sclerosing cholangitis, autoimmune hepatitis and hemochromatosis. NASH/NAFLD, non-alcoholic steatohepatitis/non-alcoholic fatty liver disease; RFA, radiofrequency ablation; TACE, transarterial chemoembolization; SIRT, selective internal radiation therapy; INR, international normalized ratio; CRP, C-reactive protein; Na^+, sodium; Cr, creatinine; AFP, α-fetoprotein; ECOG, Eastern Cooperative Oncology Group; BCLC, Barcelona Clinic Liver Cancer staging system; IQR, interquartile range.

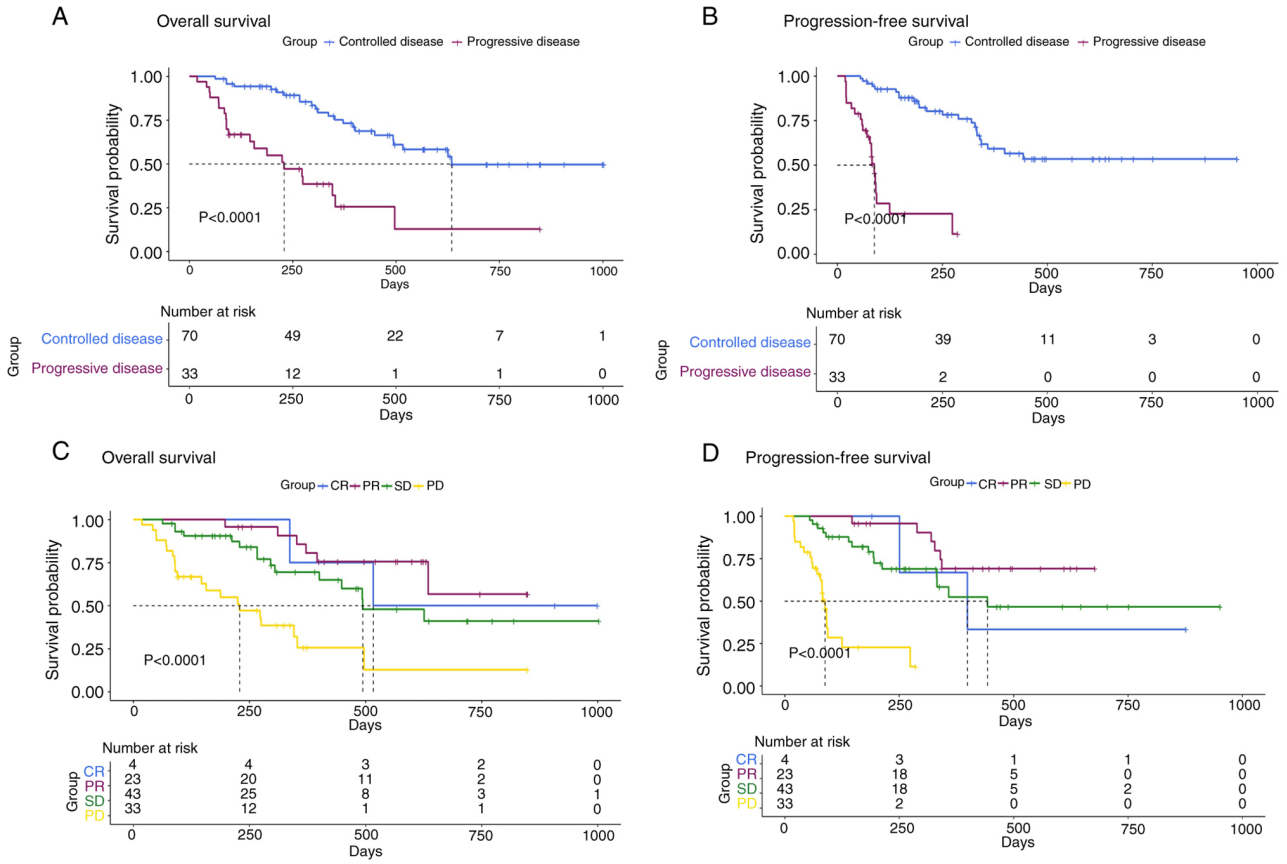

Figure 1. Overall and progression-free survival. Survival curves: (A and C) Overall and (B and D) progression-free survival according to (A and B) control vs. progression and (C and D) modified Response Evaluation Criteria on Solid Tumors category. CR, complete response; PD, disease progression; PR, partial response; SD, stable disease.

Table II. Response to therapy and survival.

Variable	Disease control	Progressive disease	P-value
Reason for discontinuation of therapy, n (%)			$7.423x10^{-8}$
Still ongoing	23 (32.9)	0 (0.0)	
Radiological progression	15 (21.4)	24 (72.7)	
Adverse event	4 (5.7)	0 (0.0)	
Clinical deterioration	10 (14.3)	3 (9.1)	
Death	7 (10.0)	6 (18.2)	
Other	11 (15.7)	0 (0.0)	
mRECIST after 3 months of atezolizumab/ bevacizumab, n (%)			$1.050x10^{-27}$
Complete response	4 (5.7)	0 (0.0)	
Partial response	23 (32.9)	0 (0.0)	
Stable disease	43 (61.4)	0 (0.0)	
Progressive disease	0 (0.0)	33 (100.0)	
Median progression-free survival in days (IQR)	280.50 (169.00, 445.25)	81.00 (56.00, 89.00)	<0.001
Median overall survival in days (IQR)	381.50 (226.75, 568.50)	147.00 (90.00, 309.00)	<0.001
Death (yes), n (%)	23 (32.9)	21 (63.6)	0.005

IQR, interquartile range; mRECIST, modified Response Evaluation Criteria on Solid Tumors.

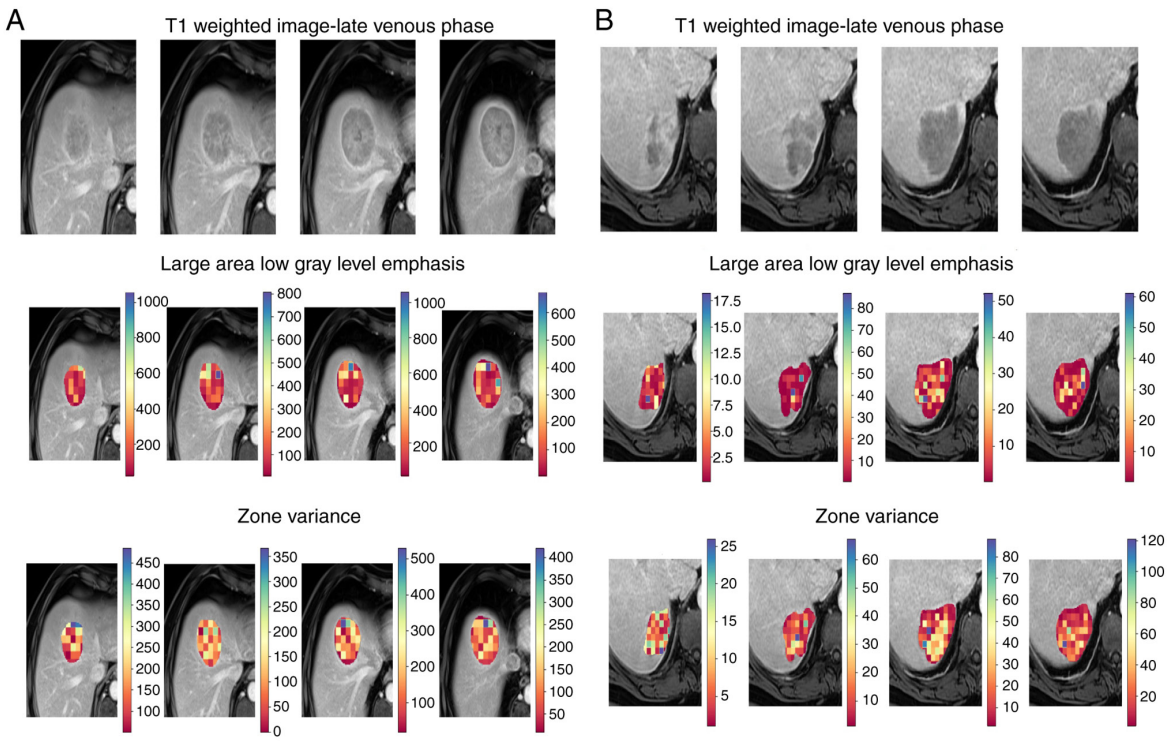

Figure 2. Radiomics features represented as a heatmap in the ROI. Example of a radiomics heatmap in (A) a 62-year-old male patient who responded to therapy and survived for at least 484 days after the beginning of atezolizumab and bevacizumab treatment and (B) a 70-year-old male patient who progressed in spite of therapy but still survived at least 266 days after the beginning of immunotherapy. The ROI corresponds to a hepatocellular carcinoma tumor and the radiomics features depicted are: Large area low gray level emphasis, which highlights regions of large, low-intensity areas, with high values indicating homogeneous, low-contrast zones; and zone variance, which measures the variability in zone sizes, where high values suggest greater heterogeneity in texture, while low values reflect more uniform zone sizes. ROI, region of interest.

protein, metastases, previous systemic therapy, and absence of TACE (Fig. 3B). The clinical model achieved 82% accuracy and an ROC AUC of 0.896 with 48% sensitivity and 98.1% specificity on the training set, and 73% accuracy and an ROC AUC of 0.649 with 25% sensitivity and 94.4% specificity on the test set (Fig. 4B).

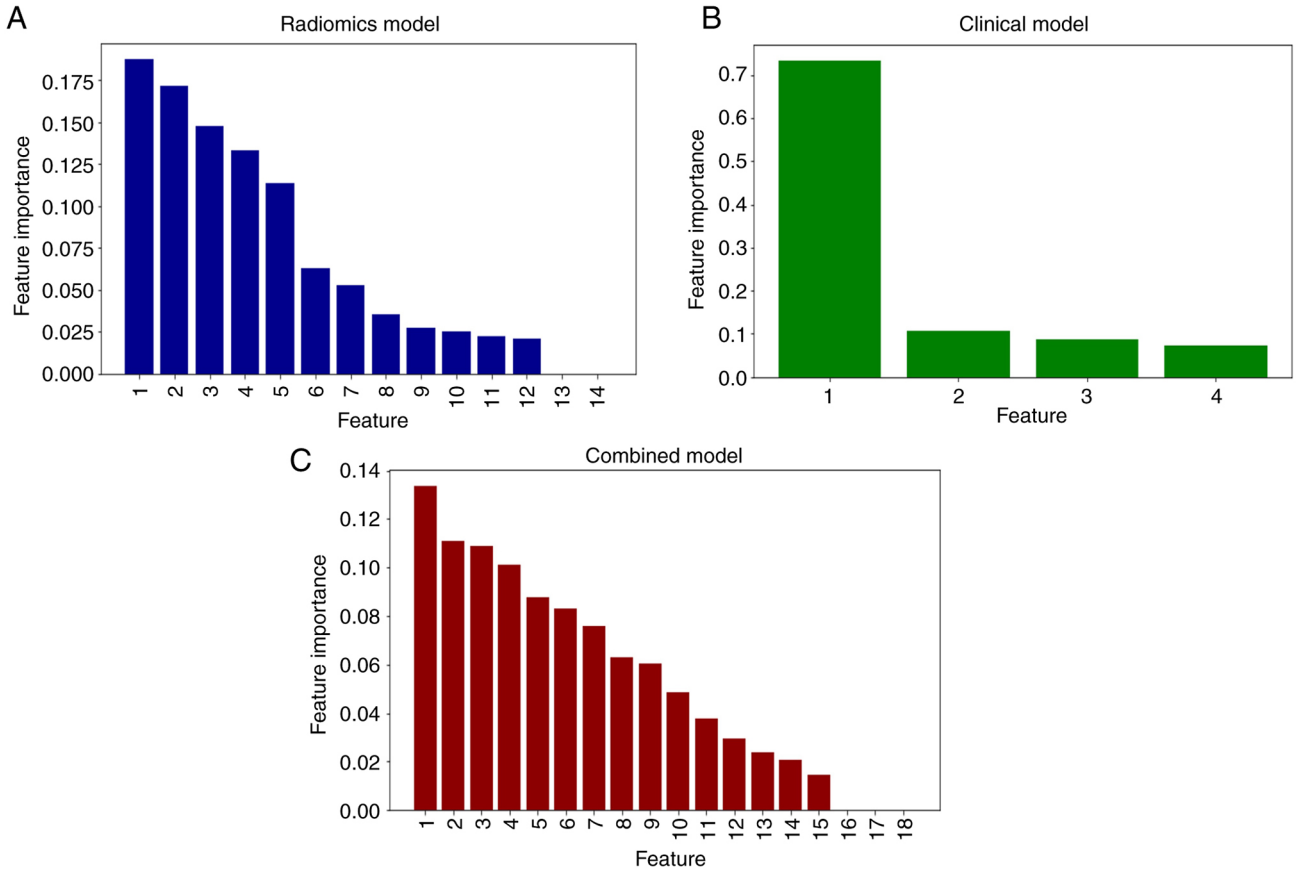

Figure 3. Feature importance in the different models. (A) Radiomics model. 1, GLSZM large area low gray level emphasis; 2, GLCM cluster shade; 3, GLSZM zone variance; 4, GLSZM large area high gray level emphasis; 5, GLCM joint average; 6, first order skewness; 7, GLSZM large area emphasis; 8, GLRLM short run high gray level emphasis; 9, GLRLM long run low gray level emphasis; 10, GLCM autocorrelation; 11, GLCM sum average; 12, GLSZM low gray level zone emphasis; 13, GLRLM high gray level run emphasis; and 14, GLDM high gray level emphasis. (B) Clinical model. 1, C-reactive protein; 2, metastasis status; 3, previous systemic therapy; and 4, previous TACE. (C) Combined model. 1, GLSZM zone variance; 2, GLSZM large area high gray level emphasis; 3, GLRLM high gray level run emphasis; 4, GLDM high gray level emphasis; 5, GLRLM long run low gray level emphasis; 6, GLCM joint average; 7, GLCM autocorrelation; 8, first order skewness; 9, GLRLM short run high gray level emphasis; 10, GLSZM low gray level zone emphasis; 11, previous systemic therapy; 12, metastasis status; 13, GLCM sum average; 14, C-reactive protein; 15, GLSZM large area emphasis; 16, GLSZM large area low gray level emphasis; 17, GLCM cluster shade; and 18, previous TACE. GLCM, gray level co-occurrence matrix; GLDM, gray level dependence matrix; GLRLM, gray level run length matrix; GLSZM, gray level size zone matrix; TACE, transarterial chemoembolization.

Combined model. A combined feature set was created by merging selected radiomics (14 features) and clinical (4 features) datasets, resulting in an 18-feature model (Fig. 3C). The RandomForestClassifier was again employed, achieving 82% accuracy and an ROC AUC of 0.911 with 52% sensitivity and 96% specificity on the training set, and 69% accuracy and an ROC AUC of 0.753 with 12.5% sensitivity and 94.4% specificity on the test set (Fig. 4C).

The model was reevaluated using the following parameters obtained from hyperparameter tuning: 3 estimators, 'log2' for max features, max depth of 5, minimum samples split of 2, minimum samples leaf of 4, 'gini' criterion, and no bootstrap. The final performance achieved an accuracy of 92.2% and ROC-AUC of 0.976 for the training set, and an accuracy of 80.1% and ROC-AUC of 0.771 for the testing set (Fig. 5). All relevant metrics of the different models are summarized in Table III.

Discussion

The introduction of the combination therapy of atezolizumab/bevacizumab has marked a significant milestone in the treatment landscape of HCC (6,7). Despite the notable advancements, a subset of patients still faces challenges with suboptimal treatment response. In the context of evolving additional therapeutic options such as durvalumab/tremelimumab (12), camrelizumab/rivoceranib (14), and nivolumab/ipilimumab (13), selection criteria of patients benefiting from a specific treatment are becoming increasingly important for optimizing patient outcomes.

With the publication of the IMbrave150 trial and a weaker performance of atezolizumab/bevacizumab in the subgroup of non-viral HCCs, discussions about subgroups and their benefit from treatments began (7). The effect in patients with HCC of non-viral etiology is commonly discussed after a subgroup analysis of the IMbrave150 study failed to prove extended OS in those patients compared to sorafenib (7,11). A subsequent meta-analysis supported the use of atezolizumab/bevacizumab in those patients, but the underlying data were highly variable (18). Another study has demonstrated the superiority of lenvatinib over the combined treatment in patients with metabolic etiology (19). A weak performance of atezolizumab/bevacizumab in non-viral HCC was further

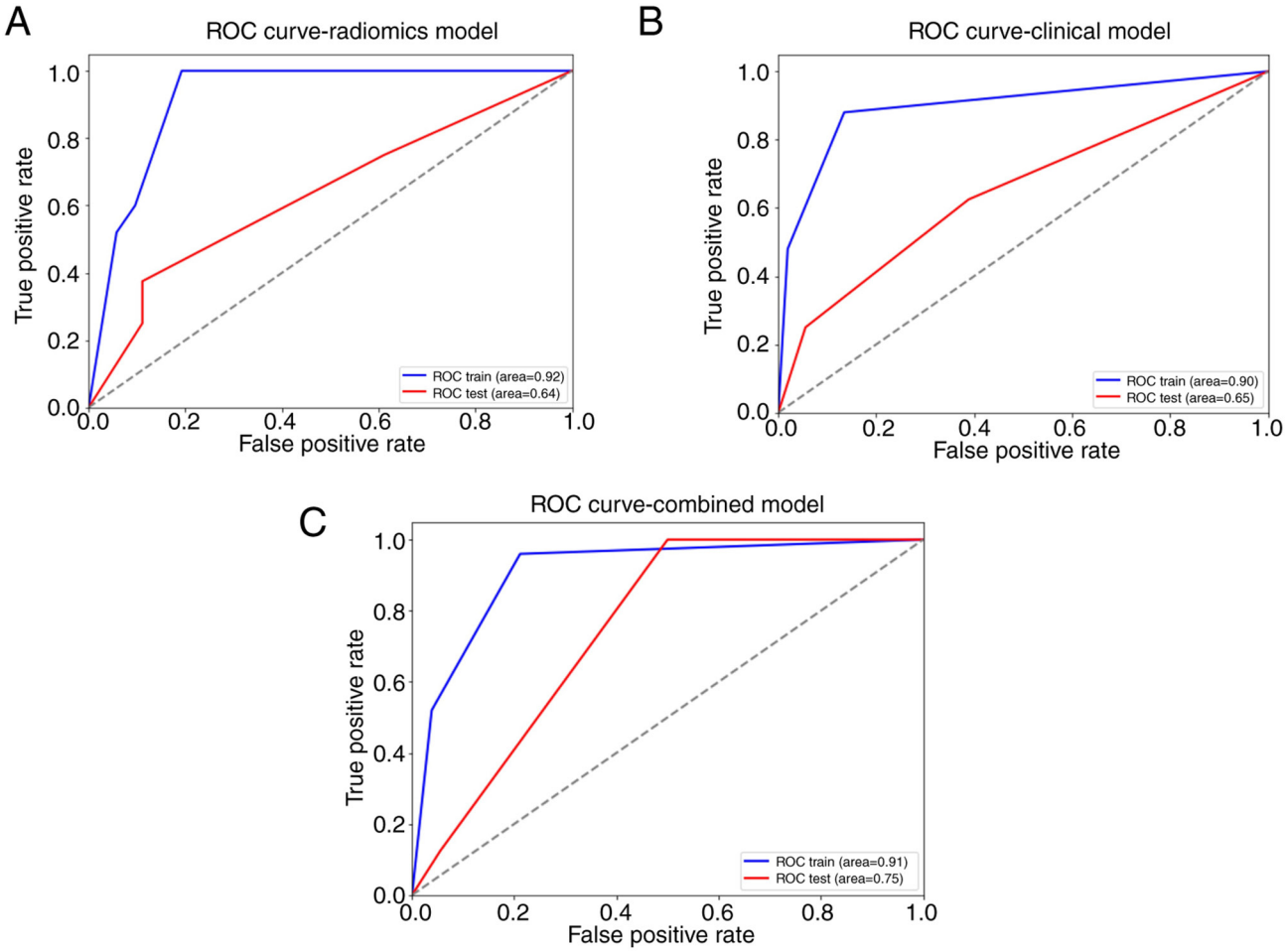

Figure 4. ROC curves for each of the different models. ROC curves for the (A) radiomics, (B) clinical and (C) combined models. ROC, receiver operating characteristic.

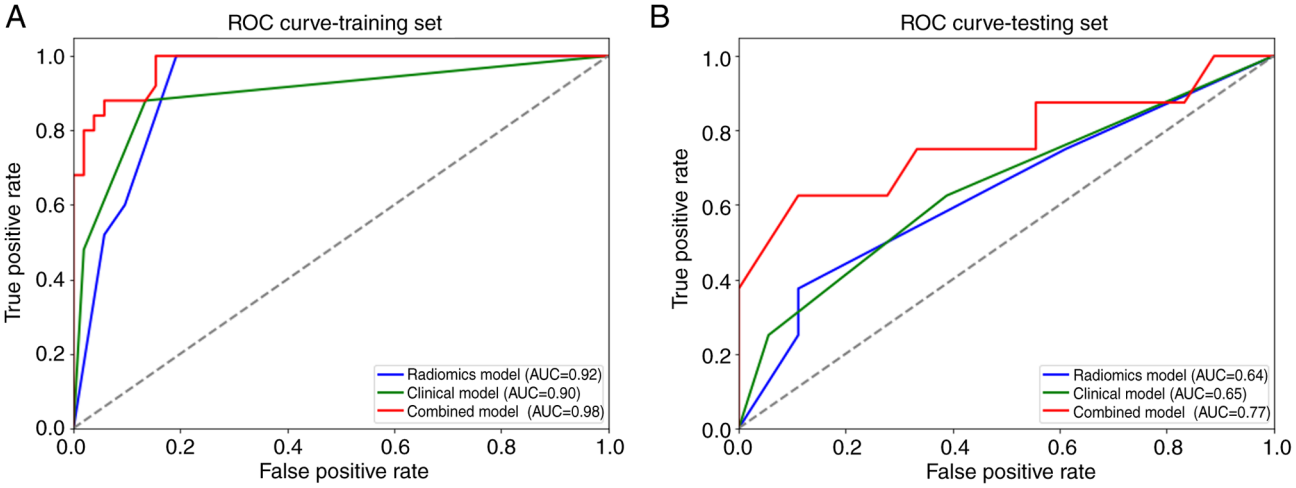

Figure 5. ROC curves after hyperparameter tuning. ROC curves of the (A) training set and (B) testing set after hyperparameter tuning. For the combined model, the AUC was 0.77 in the testing set, with an accuracy of 80.1%, sensitivity of 62.5% and specificity of 89%. AUC, area under the curve; ROC, receiver operating characteristic.

substantiated by Pfister and colleagues demonstrating similar findings in a murine cancer model (20). In contrast, durvalumab/tremelimumab performed well in non-viral HCCs, even further widening room for discussion on subgroup-specific treatment of HCC (12,21). While non-viral HCCs tend to exhibit greater tumor heterogeneity and distinct tumor microenvironment features, whether these factors are associated with a poorer response to atezolizumab/bevacizumab

Table III. Metrics of the different models in the training and testing sets.

	Training set			Testing set		
Metric	Radiomics model	Clinical model	Combined model[a]	Radiomics model	Clinical model	Combined model[a]
Accuracy	0.81	0.82	0.82/0.92	0.73	0.73	0.69/0.81
ROC AUC	0.9212	0.8965	0.9108/0.9757	0.6354	0.6493	0.7535/0.7708
Sensitivity	0.6000	0.4800	0.5200/0.8000	0.3750	0.2500	0.1250/0.6250
Specificity	0.9038	0.9808	0.9615/0.9800	0.8889	0.9444	0.9444/0.8900
PPV	0.7500	0.9231	0.8667/0.9500	0.6000	0.6667	0.5000/0.7140
NPV	0.8246	0.7969	0.8065/0.9100	0.7619	0.7391	0.7083/0.8420

[a]Before/after hyperparameter tuning. ROC, receiver operating characteristic; AUC, area under the curve; PPV, positive predictive value; NPV, negative predictive value.

compared to durvalumab/tremelimumab or sorafenib remains to be elucidated (18-21).

Just recently, additional subgroup analyses from the HIMALAYA trial underscored the potential utility of irAEs as predictive biomarkers for treatment response and prognosis in HCC patients treated with durvalumab/tremelimumab (22). Subsequently, similar results were also demonstrated for atezolizumab/bevacizumab (23). However, as these irAEs occur only after initiation of treatment, they are not useful for primary selection of treatment efficacy in HCC patients.

Given the difference in response to atezolizumab/bevacizumab, several attempts have been made to apply serum markers and scores to predict the efficacy of immunotherapy in HCC. For example, a low pretreatment neutrophil-to-lymphocyte ratio (NLR) has been associated with significantly longer PFS and OS (8,24). The CRAFITY (CRP and AFP in immunotherapy) score demonstrated a pretreatment AFP ≥100 ng/ml and/or C-reactive protein (CRP) ≥1 mg/dl to be correlated with worse survival and progression of HCC (25). The IMABALI-De (AFP, BCLC staging, mALBI, and DCP evaluation (IMABALI-De) scoring model was suggested to be superior to the CRAFITY score for both OS and PFS (26). Recently, Gairing and colleagues proposed the CABLE score, consisting of C-reactive protein, albumin, bilirubin, lymphocytes, ECOG performance status, and extrahepatic spread (27). Nevertheless, independent evaluation is also missing for these scores. Thus, despite multiple other efforts to establish clinically meaningful methods to predict treatment response of immunotherapy in HCC, none of those scores was further pursued in clinical trials or even independent validation attempts (28-30).

In order to validate the clinical features of our model, we ranked them according to their importance. The top-ranked factors were C-reactive protein, presence of metastases at the beginning of therapy, previous treatment with systemic therapy, particularly sorafenib, and absence of TACE. CRP has previously been identified as an independent prognostic factor in multivariable analysis (25) and thus, our analysis reaffirms its importance. For the other three clinical variables, the proportion of patients was considerably unfavorable for the PD group, suggesting worse baseline parameters compared to the DC group, accounting for a worse prognosis.

However, since serum markers and demographic variables have thus far failed to provide sufficient prediction of response to atezolizumab/bevacizumab for the treatment of HCC, we aimed to explore other options, particularly radiomics strategies. Radiomics has been repeatedly proven to hold immense potential to revolutionize cancer diagnosis and management by leveraging the wealth of information contained within medical images (31-33). In HCC, radiomics has been utilized to predict various factors such as microvascular invasion and expression of markers like Ki67 (34-38). Nonetheless, its application to predict the outcome of immunotherapy in liver cancer is novel and represents an exciting frontier in cancer research.

In our radiomics model, all but one radiomic feature were textural features, which have proved to be valuable in assessing the internal heterogeneity of tumors and are frequently used in studies aiming to predict treatment response. So far, textural features extracted from dynamic contrast-enhanced MRI in HCC patients have been utilized to predict microvascular invasion (39), tumor grading (40), and pathological differentiation (41). The first study emphasized that dynamic changes in textural features over different MRI phases (e.g., arterial to portal vein phase) were particularly useful for prediction while the last study highlighted both intratumoral and peritumoral textural features like GLCM dissimilarity, entropy, and contrast, along with GLRLM short-run emphasis and GLSZM zone entropy as key discriminators.

Since none of the previous models have reached sufficient performance to predict response to therapy, we decided to investigate the addition of radiomics features to our model as a hybrid approach. Hybrid models, combining clinical with radiological qualitative characteristics (e.g. pseudocapsule, two-trait predictor of venous invasion, and peritumoral enhancement) have emerged as a promising strategy for preoperative prediction of microvascular invasion and therefore help predict surgical outcomes from CT images (37,38). Furthermore, MRI-based radiomic scores have demonstrated utility in predicting microvascular invasion and response to TACE, particularly when complemented by additional clinical parameters such as AFP levels, Child-Pugh score,

and BCLC stage (34,42). Moreover, it has been evidenced that high intensity in the hepatobiliary phase of Gd-EOB-DTPA-enhanced MRI is associated with β-catenin activation as well as unfavorable response to anti-PD1 antibodies (43).

To the best of our knowledge, there is no study linking baseline-MRI radiomics features to response to atezolizumab/bevacizumab and thus, there are no predictive radiomics biomarkers for immunotherapy treatment in HCC (44). Overall, only a few studies have approached the task of evaluating radiomic profiles in predicting the efficacy of immunotherapy and most of these studies achieved AUCs between 0.69 and 0.82 (45). The best-performing model seems to be the one recently reported by Dercle *et al* (46), who assessed melanoma treatment efficacy with ipilimumab/pembrolizumab vs. pembrolizumab alone and were able to outperform RECIST in predicting OS, with an AUC of 0.92 (95% CI: 0.89-0.95). However, this study was also controversial due to a lack of detailed information on CT acquisition parameters, radiomics feature extraction platform, preprocessing steps, and model details (45).

Combining clinical and radiomics features in a hybrid model we reached a final accuracy of 80.1% and AUC of 0.771 for the testing set. However, we acknowledge that our study has certain limitations. While the multicentric approach for this study was needed to achieve the necessary number of patients, it also poses the risk of a certain heterogeneity of acquired imaging data. This risk was mitigated by, first, only including patients with a dedicated contrast-enhanced MRI for the liver (including image preprocessing before feature extraction) and, second, a reading of the cases by a radiologist with experience in oncologic imaging for image quality before inclusion. Furthermore, the response assessment itself may be discussed critically: this study performed a response assessment based on mRECIST compared to the partly still utilized RECIST 1.1 criteria for response assessment. While this may partly hamper compatibility, the choice in favor of mRECIST was taken based on published evidence: a meta-analysis (47) based on 23 studies with a total of 2574 patients concludes, that mRECIST may be more accurate than classical RECIST in the setting of molecular targeted therapies in HCC.

An important limitation of our study is represented by the dataset's class imbalance, with 70 patients achieving disease control and only 33 experiencing disease progression, which significantly impacted the accuracy, sensitivity, and AUC on the test set. The 75:25 train-test split further reduced the number of progression cases in the test set, making it difficult for the model to accurately classify this minority class. Consequently, sensitivity dropped to 37.5% for the radiomics model and even lower for the clinical (25%) and combined (12.5%) models, indicating a tendency to misclassify progression cases as disease control.

However, the improvement in accuracy and AUC after hyperparameter tuning supports the effectiveness of our pipeline in identifying new biomarkers capable of predicting response to emerging HCC therapies using advanced diagnostic methods, such as machine learning. An estimated number of sixty additional patients in the PD group and seventy in the DC would help address the class imbalance, and an external validation cohort would ensure the robustness and applicability of our model, providing important future directions for our research.

In conclusion, our hybrid model combining traditional clinical and serological markers with radiological qualitative characteristics resulted in a model with a better accuracy in predicting response to atezolizumab/bevacizumab in patients with HCC. The hybrid model outperformed models solely based on clinical/serological parameters or radiomics features.

Acknowledgements

This abstract was presented at the Annual Meeting of the German Association for the Study of the Liver (January 27, 2024; Essen, Germany), and was published as Abstract no. 10.1055/s-0043-1777615. This abstract was also presented at the Viszeralmedizin 2024 Congress of the Deutsche Gesellschaft für Gastroenterologie, Verdauungs- und Stoffwechselkrankheiten (German Association for Gastroenterology, Digestive and Metabolic Diseases; October 4, 2024; Leipzig, Germany), and was published as Abstract no. 10.1055/s-0044-1789914.

The authors would like to thank Miss Anja Zinke (Department of Radiology and Nuclear Medicine, Magdeburg University, Magdeburg, Germany) for providing technical support in loading the images. The authors would also like to thank Dr Laura Santamaria (School of Medicine, University of the Andes, Bogota, Colombia) for their contributions during their internship (at Department of Medicine II, Medical Faculty Mannheim, Heidelberg University, Mannheim, Germany), where they helped to organize the structure of several sections of the manuscript.

Funding

No funding was received.

Availability of data and materials

The data generated in the present study may be requested from the corresponding author.

Authors' contributions

AT and MFF confirmed the authenticity of all the raw data. AT, MFF and MPE conceived the idea and supervised the final draft. MVá wrote and edited the manuscript, designed the figures and was involved in the statistical analysis. IR collected all the clinical and radiological data, performed the statistical analysis, wrote the manuscript, edited it and handled formatting. AV, TI and JD contributed to the statistical analysis. DHC, MD, MS, SOS, LM, DT, FS, MPe and MFF collected, anonymized and prepared the MRI data from their respective centers. MTD, JM, SM, PRG, AW, DT, MPi, BS, FS, VK and MVe identified the patients in their corresponding centers and gathered the clinical data. All authors read and approved the final version of the manuscript.

Ethics approval and consent to participate

The present study was approved by the Ethik-Kommission II der Universität Heidelberg, Mannheim, Germany, with number 2022-807, to be implemented in Mannheim and subsequently

amended to include the other centers. Given that the study did not involve any risk or change in the therapy delivered to the patients, the ethics committee determined that individual patient consent to participate was not required. In accordance with ethical guidelines, the data were anonymized, ensuring that no personal identifiers are disclosed, thus maintaining the confidentiality and privacy of all participants.

Patient consent for publication

The present study was conducted as a retrospective analysis, which involved the collection and review of previously recorded data. The study was approved by the ethics committee (Ethik-Kommission II der Universität Heidelberg; approval no. 2022-807). Given that the study does not involve the publication of any identifying patient information, the ethics committee has determined that individual patient consent for publication is not required. In accordance with ethical guidelines, the data were anonymized, ensuring that no personal identifiers are disclosed, thus maintaining the confidentiality and privacy of all participants.

Competing interests

The authors declare that they have no competing interests.

References

1. McGlynn KA, Petrick JL and El-Serag HB: Epidemiology of hepatocellular carcinoma. Hepatology 73 (Suppl 1): S4-S13, 2021.
2. Schütte K, Kipper M, Kahl S, Bornschein J, Götze T, Adolf D, Arend J, Seidensticker R, Lippert H, Ricke J and Malfertheiner P: Clinical characteristics and time trends in etiology of hepatocellular cancer in Germany. Digestion 87: 147-159, 2013.
3. Llovet J, Brú C and Bruix J: Prognosis of hepatocellular carcinoma: The BCLC staging classification. Semin Liver Dis 19: 329-338, 1999.
4. Reig M, Forner A, Rimola J, Ferrer-Fàbrega J, Burrel M, Garcia-Criado Á, Kelley RK, Galle PR, Mazzaferro V, Salem R, *et al*: BCLC strategy for prognosis prediction and treatment recommendation: The 2022 update. J Hepatol 76: 681-693, 2022.
5. Benson AB, D'Angelica MI, Abbott DE, Anaya DA, Anders R, Are C, Bachini M, Borad M, Brown D, Burgoyne A, *et al*: Hepatobiliary cancers, version 2.2021, NCCN clinical practice guidelines in oncology. J Natl Compr Canc Netw 19: 541-565, 2021.
6. Vogel A and Martinelli E; ESMO Guidelines Committee. Electronic address: clinicalguidelines@esmo.org; ESMO Guidelines Committee: Updated treatment recommendations for hepatocellular carcinoma (HCC) from the ESMO clinical practice guidelines. Ann Oncol 32: 801-805, 2021.
7. Finn RS, Qin S, Ikeda M, Galle PR, Ducreux M, Kim TY, Kudo M, Breder V, Merle P, Kaseb AO, *et al*: Atezolizumab plus bevacizumab in unresectable hepatocellular carcinoma. N Engl J Med 382: 1894-1905, 2020.
8. Jost-Brinkmann F, Demir M, Wree A, Luedde T, Loosen SH, Müller T, Tacke F, Roderburg C and Mohr R: Atezolizumab plus bevacizumab in unresectable hepatocellular carcinoma: Results from a German real-world cohort. Aliment Pharmacol Ther 57: 1313-1325, 2023.
9. Jun CH, Yoon JH, Cho E, Shin SS, Cho SB, Kim HJ, Park CH, Kim HS, Choi SK and Rew JS: Barcelona clinic liver cancer-stage C hepatocellular carcinoma: A novel approach to subclassification and treatment. Medicine (Baltimore) 96: e6745, 2017.
10. Salem R, Li D, Sommer N, Hernandez S, Verret W, Ding B and Lencioni R: Characterization of response to atezolizumab + bevacizumab versus sorafenib for hepatocellular carcinoma: Results from the IMbrave150 trial. Cancer Med 10: 5437-5447, 2021.
11. Cheng AL, Qin S, Ikeda M, Galle PR, Ducreux M, Kim TY, Lim HY, Kudo M, Breder V, Merle P, *et al*: Updated efficacy and safety data from IMbrave150: Atezolizumab plus bevacizumab vs sorafenib for unresectable hepatocellular carcinoma. J Hepatol 76: 862-873, 2022.
12. Abou-Alfa GK, Lau G, Kudo M, Chan SL, Kelley RK, Furuse J, Sukeepaisarnjaroen W, Kang YK, Van Dao T, De Toni EN, *et al*: Tremelimumab plus durvalumab in unresectable hepatocellular carcinoma. NEJM Evid 1: EVIDoa2100070, 2022.
13. Bristol Myers Squibb: Bristol myers squibb announces checkmate-9DW trial evaluating opdivo (nivolumab) plus yervoy (ipilimumab) meets primary endpoint of overall survival for the first-line treatment of advanced hepatocellular carcinoma. https://news.bms.com/news/details/2024/Bristol-Myers-Squibb-Announces-CheckMate--9DW-Trial-Evaluating-Opdivo-nivolumab-Plus-Yervoy-ipilimumab-Meets-Primary-Endpoint-of-Overall-Survival-for-the-First-Line-Treatment-of-Advanced-Hepatocellular-Carcinoma/default.aspx.
14. Qin S, Chan SL, Gu S, Bai Y, Ren Z, Lin X, Chen Z, Jia W, Jin Y, Guo Y, *et al*: Camrelizumab plus rivoceranib versus sorafenib as first-line therapy for unresectable hepatocellular carcinoma (CARES-310): A randomised, open-label, international phase 3 study. Lancet 402: 1133-1146, 2023.
15. Lencioni R and Llovet J: Modified RECIST (mRECIST) assessment for hepatocellular carcinoma. Semin Liver Dis 30: 52-60, 2010.
16. Fedorov A, Beichel R, Kalpathy-Cramer J, Finet J, Fillion-Robin JC, Pujol S, Bauer C, Jennings D, Fennessy F, Sonka M, *et al*: 3D Slicer as an image computing platform for the quantitative imaging network. Magn Reson Imaging 30: 1323-1341, 2012.
17. Van Griethuysen JJM, Fedorov A, Parmar C, Hosny A, Aucoin N, Narayan V, Beets-Tan RGH, Fillion-Robin JC, Pieper S and Aerts HJWL: Computational radiomics system to decode the radiographic phenotype. Cancer Res 77: e104-e107, 2017.
18. Vogel A, Rimassa L, Sun HC, Abou-Alfa GK, El-Khoueiry A, Pinato DJ, Sanchez Alvarez J, Daigl M, Orfanos P, Leibfried M, *et al*: Comparative efficacy of atezolizumab plus bevacizumab and other treatment options for patients with unresectable hepatocellular carcinoma: A network meta-analysis. Liver Cancer 10: 240-248, 2021.
19. Rimini M, Rimassa L, Ueshima K, Burgio V, Shigeo S, Tada T, Suda G, Yoo C, Cheon J, Pinato DJ, *et al*: Atezolizumab plus bevacizumab versus lenvatinib or sorafenib in non-viral unresectable hepatocellular carcinoma: An international propensity score matching analysis. ESMO Open 7: 100591, 2022.
20. Pfister D, Núñez NG, Pinyol R, Govaere O, Pinter M, Szydlowska M, Gupta R, Qiu M, Deczkowska A, Weiner A, *et al*: NASH limits anti-tumour surveillance in immunotherapy-treated HCC. Nature 592: 450-456, 2021.
21. Sangro B, Chan SL, Kelley RK, Lau G, Kudo M, Sukeepaisarnjaroen W, Yarchoan M, De Toni EN, Furuse J, Kang YK, *et al*: Four-year overall survival update from the phase III HIMALAYA study of tremelimumab plus durvalumab in unresectable hepatocellular carcinoma. Ann Oncol 35: 448-457, 2024.
22. Lau G, Sangro B, Crysler OV, Sukeepaisarnjaroen W, Lipatov O, Morimoto M, Archambeaud I, Burgio V, Phuong LTT, Chao T, *et al*: Temporal patterns of immune-mediated adverse events (imAEs) with tremelimumab (T) plus durvalumab (D) in the phase 3 HIMALAYA study in unresectable hepatocellular carcinoma (uHCC). J Clin Oncol 41 (16 Suppl): S4073, 2023.
23. Fukushima T, Morimoto M, Kobayashi S, Ueno M, Uojima H, Hidaka H, Kusano C, Chuma M, Numata K, Tsuruya K, *et al*: Association between immune-related adverse events and survival in patients with hepatocellular carcinoma treated with atezolizumab plus bevacizumab. Oncologist 28: e526-e533, 2023.
24. Eso Y, Takeda H, Taura K, Takai A, Takahashi K and Seno H: Pretreatment neutrophil-to-lymphocyte ratio as a predictive marker of response to atezolizumab plus bevacizumab for hepatocellular carcinoma. Curr Oncol 28: 4157-6416, 2021.
25. Scheiner B, Pomej K, Kirstein MM, Hucke F, Finkelmeier F, Waidmann O, Himmelsbach V, Schulze K, von Felden J, Fründt TW, *et al*: Prognosis of patients with hepatocellular carcinoma treated with immunotherapy-development and validation of the CRAFITY score. J Hepatol 76: 353-363, 2022.
26. Ohama H, Hiraoka A, Tada T, Hirooka M, Kariyama K, Hatanaka T, Tani J, Takaguchi K, Atsukawa M, Itobayashi E, *et al*: Clinical usefulness of newly developed prognostic predictive score for atezolizumab plus bevacizumab for hepatocellular carcinoma. Cancer Rep (Hoboken) 7: e2042, 2024.

27. Gairing SJ: Development and validation of the CABLE score to estimate individual prognosis of patients with hepatocellular carcinoma treated with 1L atezolizumab and bevacizumab. In: Proceedings of the EASL Progress. EASL, Milan, 2024. https://www.easlcongress.eu/wp-content/uploads/2024/03/List-of-accepted-abstracts-EASL-Congress-2024_new.pdf.
28. Hatanaka T, Kakizaki S, Hiraoka A, Tada T, Hirooka M, Kariyama K, Tani J, Atsukawa M, Takaguchi K, Itobayashi E, *et al*: Development and validation of a modified albumin-bilirubin grade and α-fetoprotein score (mALF score) for hepatocellular carcinoma patients receiving atezolizumab and bevacizumab. Hepatol Int 17: 86-96, 2023.
29. Hiraoka A, Kumada T, Tada T, Hirooka M, Kariyama K, Tani J, Atsukawa M, Takaguchi K, Itobayashi E, Fukunishi S, *et al*: Geriatric nutritional risk index as an easy-to-use assessment tool for nutritional status in hepatocellular carcinoma treated with atezolizumab plus bevacizumab. Hepatol Res 53: 1031-1042, 2023.
30. Tada T, Kumada T, Hiraoka A, Kariyama K, Tani J, Hirooka M, Takaguchi K, Atsukawa M, Fukunishi S, Itobayashi E, *et al*: New prognostic system based on inflammation and liver function predicts prognosis in patients with advanced unresectable hepatocellular carcinoma treated with atezolizumab plus bevacizumab: A validation study. Cancer Med 12: 6980-6993, 2023.
31. Bera K, Braman N, Gupta A, Velcheti V and Madabhushi A: Predicting cancer outcomes with radiomics and artificial intelligence in radiology. Nat Rev Clin Oncol 19: 132-146, 2022.
32. Gillies RJ and Schabath MB: Radiomics improves cancer screening and early detection. Cancer Epidemiol Biomarkers Prev 29: 2556-2567, 2020.
33. Lambin P, Rios-Velazquez E, Leijenaar R, Carvalho S, Van Stiphout RGPM, Granton P, Zegers CM, Gillies R, Boellard R, Dekker A and Aerts HJ: Radiomics: Extracting more information from medical images using advanced feature analysis. Eur J Cancer 48: 441-446, 2012.
34. Chong HH, Yang L, Sheng RF, Yu YL, Wu DJ, Rao SX, Yang C and Zeng MS: Multi-scale and multi-parametric radiomics of gadoxetate disodium-enhanced MRI predicts microvascular invasion and outcome in patients with solitary hepatocellular carcinoma ≤5 cm. Eur Radiol 31: 4824-4838, 2021.
35. Gong XQ, Tao YY, Wu Y, Liu N, Yu X, Wang R, Zheng J, Liu N, Huang XH, Li JD, *et al*: Progress of MRI radiomics in hepatocellular carcinoma. Front Oncol 11: 698373, 2021.
36. Li Y, Yan C, Weng S, Shi Z, Sun H, Chen J, Xu X, Ye R and Hong J: Texture analysis of multi-phase MRI images to detect expression of Ki67 in hepatocellular carcinoma. Clin Radiol 74: 813.e19-813.e27, 2019.
37. Xia TY, Zhou ZH, Meng XP, Zha JH, Yu Q, Wang WL, Song Y, Wang YC, Tang TY, Xu J, *et al*: Predicting microvascular invasion in hepatocellular carcinoma using CT-based radiomics model. Radiology 307: e222729, 2023.
38. Xu X, Zhang HL, Liu QP, Sun SW, Zhang J, Zhu FP, Yang G, Yan X, Zhang YD and Liu XS: Radiomic analysis of contrast-enhanced CT predicts microvascular invasion and outcome in hepatocellular carcinoma. J Hepatol 70: 1133-1144, 2019.
39. Zhang R, Wang Y, Li Z, Shi Y, Yu D, Huang Q, Chen F, Xiao W, Hong Y and Feng Z: Dynamic radiomics based on contrast-enhanced MRI for predicting microvascular invasion in hepatocellular carcinoma. BMC Med Imaging 24: 80, 2024.
40. Wu M, Tan H, Gao F, Hai J, Ning P, Chen J, Zhu S, Wang M, Dou S and Shi D: Predicting the grade of hepatocellular carcinoma based on non-contrast-enhanced MRI radiomics signature. Eur Radiol 29: 2802-2811, 2019.
41. Liu HF, Wang M, Wang Q, Lu Y, Lu YJ, Sheng Y, Xing F, Zhang JL, Yu SN and Xing W: Multiparametric MRI-based intratumoral and peritumoral radiomics for predicting the pathological differentiation of hepatocellular carcinoma. Insights Imaging 15: 97, 2024.
42. Kong C, Zhao Z, Chen W, Lv X, Shu G, Ye M, Song J, Ying X, Weng Q, Weng W, *et al*: Prediction of tumor response via a pretreatment MRI radiomics-based nomogram in HCC treated with TACE. Eur Radiol 31: 7500-7511, 2021.
43. Aoki T, Nishida N, Ueshima K, Morita M, Chishina H, Takita M, Hagiwara S, Ida H, Minami Y, Yamada A, *et al*: Higher enhancement intrahepatic nodules on the hepatobiliary phase of Gd-EOB-DTPA-enhanced MRI as a poor responsive marker of anti-PD-1/PD-L1 monotherapy for unresectable hepatocellular carcinoma. Liver Cancer 10: 615-628, 2021.
44. Tamura Y, Ono A, Nakahara H, Hayes CN, Fujii Y, Zhang P, Yamauchi M, Uchikawa S, Teraoka Y, Uchida T, *et al*: Association of hepatobiliary phase of gadoxetic-acid-enhanced MRI imaging with immune microenvironment and response to atezolizumab plus bevacizumab treatment. Cancers (Basel) 15: 4234, 2023.
45. Kothari G: Role of radiomics in predicting immunotherapy response. J Med Imaging Radiat Oncol 66: 575-591, 2022.
46. Dercle L, Zhao B, Gönen M, Moskowitz CS, Firas A, Beylergil V, Connors DE, Yang H, Lu L, Fojo T, *et al*: Early readout on overall survival of patients with melanoma treated with immunotherapy using a novel imaging analysis. JAMA Oncol 8: 385-392, 2022.
47. Yu H, Bai Y, Xie X, Feng Y, Yang Y and Zhu Q: RECIST 1.1 versus mRECIST for assessment of tumour response to molecular targeted therapies and disease outcomes in patients with hepatocellular carcinoma: A systematic review and meta-analysis. BMJ Open 12: e052294, 2022.